Available online at www.sciencedirect.com
ScienceDirect
Journal of Applied Geophysics 63 (2007) 135 – 147
JOURNAL OF APPLIED GEOPHYSICS
www.elsevier.com/locate/jappgeo

Thermal characteristics of coal fires 2: Results of measurements on simulated coal fires

Jianzhong Zhang [a], Claudia Kuenzer [a,*], Anke Tetzlaff [c], Dieter Oertel [b], Boris Zhukov [b], Wolfgang Wagner [a]

[a] *Institute of Photogrammetry and Remote Sensing (IPF), Vienna University of Technology, Gusshausstr. 27–29, A-1040 Vienna, Austria*
[b] *DLR Berlin, Optische Informationssysteme, Standort Berlin-Adlershof, Rutherfordstraße 2, 12489 Berlin, Germany*
[c] *Swedish Meteorological and Hydrological Institute, SMHI, Folkborgsvaegen 1, SE-60176 Norrkoeping, Sweden*

Received 26 November 2006; accepted 16 August 2007

Abstract

In this paper we present thermal characteristics of coal fires as measured during simulated fires under an experimental setting in Germany in July 2002. It is thus a continuation of the previously published paper "Thermal surface characteristics of coal fire 1: Results of in-situ measurement", in which we presented temperature measurements of real subsurface coal fires in China [Zhang, J., Kuenzer, C., accepted for publication. Thermal Surface Characteristics of Coal Fires 1: Results of in-situ measurements. Accepted for publication at Journal of Applied Geophysics.]. The focus is on simulated coal fires, which are less complex in nature than fires under natural conditions. In the present study we simulated all the influences usually occurring under natural conditions in a controllable manner (uniform background material of known thermal properties, known ventilation pathways, homogeneous coal substrate), creating two artificial outdoor coal fires under simplified settings. One surface coal fire and one subsurface coal fire were observed over the course of 2 days. The set up of the fires allowed for measurements not always feasible under "real" in-situ conditions: thus compared to the in-situ investigations presented in paper one we could retrieve numerous temperature measurements inside of the fires. Single temperature measurements, diurnal profiles and airborne thermal surveying present the typical temperature patterns of a small surface-and a subsurface fire under undisturbed conditions (easily accessible terrain, 24 hour measurements period, homogeneous materials). We found that the outside air temperature does not influence the fire's surface temperature (up to 900 °C), while fire centre temperatures of up to 1200 °C strongly correlate with surface temperatures of the fire. The fires could heat their surrounding up to a distance of 4.5 m. However, thermal anomalies on the background surface only persist as long as the fire is burning and disappear very fast if the heat source is removed. Furthermore, heat outside of the fires is transported mainly by convection and not by radiation. In spatial thermal line scanner data the diurnal thermal patterns of the coal fire are clearly represented. Our experiments during that data collection also visualize the thermal anomaly differences between covered (underground) and uncovered (surface) coal fires. The latter could not be observed in-situ in a real coal fire area. Sub-surface coal fires express a much weaker signal than open surface fires and contrast only by few degrees against the background. In airborne thermal imaging scanner data the fires are also well represented. Here we could show that the mid-infrared domain (3.8 μm) is more suitable to pick up very hot anomalies, compared to the common thermal (8.8 μm) domain. Our results help to

* Corresponding author. Tel./fax: +43 1 58801 12249.
E-mail addresses: jz@ipf.tuwien.ac.at (J. Zhang), ck@ipf.tuwien.ac.at (C. Kuenzer), dieter.oertel@dlr.de (D. Oertel), boris.zhukov@dlr.de (B. Zhukov), ww@ipf.tuwien.ac.at (W. Wagner).

doi:10.1016/j.jappgeo.2007.08.003

understand coal fires and their thermal patterns as well as the limitations occurring during their analysis. We believe that the results presented here can practicably help for the planning of coal fire thermal mapping campaigns — including remote sensing methods and the thermal data can be included into numerical coal fire modelling as initial or boundary conditions.

Keywords: Coal fire simulation; Simulated heat sources; Thermal analyses; Temperature profiles; Airborne thermal scanners

1. Introduction

Coal fires occur in many countries worldwide (Glover, 1998; Prakash and Gupta, 1999; Pennig, 2003; Kuenzer, 2005). A coal fire is defined as burning volume of coal, which can be a coal seam exposed to the surface, a burning underground seam or a burning coal waste or coal storage pile. The ignition of the fires can occur naturally or through human influence. In most cases coal fire ignition is triggered through mining activities (Kuenzer et al., 2007a). Through the moving and exposure of large coal volumes, reaction surfaces increase and the carbon in the coal reacts with oxygen in the air. This is an exothermal process. If the released heat cannot escape (insufficient ventilation) the coal can ignite at temperatures as low as 80 °C. (Walker 1999; Chaiken et al., 1998; Banerjee, 1982; Banerjee et al., 1972; Bylo, 1960).

Negative influences of such fires are manifold. They include the emission of large amounts of green house relevant as well as toxic and health threatening gasses (Kuenzer et al., 2007b,), the sudden collapse of bedrock due to the volume loss underground (Chen, 1997), the deterioration of vegetation, and the endangering of mining activities (see Fig. 1). Economically, they lead to the loss of the valuable resource coal. We have calculated that the loss of coal due to coal fires in China equals the German annual hard coal production (Kuenzer et al., 2007a). Accordingly, the amount of CO_2 released due to coal fires in e.g. China is estimated to contribute with 0.1% to all human induced CO_2 emissions on a global scale (Kuenzer et al., 2007a,b).

As a consequence of these devastating impacts, numerous authors have addressed the problem of coal fires based on mineralogical, geophysical and remote sensing based research. One research group mainly investigates the formation of new minerals around coal fire induced cracks and vents (Lapham et al., 1980; Coates et al., 2005, Masalehdani et al., 2005; Dai et al., 2002; Livingood et al., 1999). Other scientists employ methods such as gas sample analysis, electromagnetic profile measurements, geophysical modelling, temperature measurements, micro seismic, and geo-electrics to quantitatively analyze, locate and predict the coal fires and their development (Lohrer et al., 2005; Wessling et al., 2005; Litschke et al., 2005; Wessling, 2007. Remote sensing based coal fire research has mainly focused on coal fire related thermal anomaly detection (Ellyett and Fleming, 1974; Fisher and Knuth, 1968; Knuth et al., 1968; Giglio et al., 1999; Mansor et al., 1994; Li, 1985; Moxham and Greene, 1967; Prakash and Gupta, 1999; Prakash et al., 1995; Saraf et al., 1995; Zhang, 2004; Kuenzer et al., accepted for publication; Zhang and Kuenzer, accepted

Fig. 1. Coal fire area in Wuda, Inner Mongolia, China. Note the gas exhaust in the background of the left image. Surface fracturing and land subsidence occurs due to the volume loss underground and is commonplace. Photograph: G. Schaumann, June 2005.

for publication) the detection of land cover changes in the mining environments (Prakash and Gupta, 1998), the detection of land surface subsidence due to the volume loss underground (Guan, 1989) and the development of methods for coal fire risk area delineation (Kuenzer, 2005; Kuenzer et al., 2007c). Furthermore, in depth thermal analysis, such as sub-pixel thermal mapping (Zhang et al., 2004), geologic mapping based on emissivity (Schmugge et al., 1991) and coal fire quantification (Tetzlaff, 2004) were pursued.

Extinguishing coal fires is achieved by the depletion of the fire with oxygen (e.g. covering with sand and loess), the cooling of the fire (e.g. water injections), removal of the burning material (coal) as well as the separation of burning areas from unaffected parts of the seam with methods such as underground cement- or colloid barriers.

The objective of our experiment was to understand the thermal characteristics of coal fires (minimum-, maximum-, mean temperatures, diurnal temperature cycles, thermal anomaly extents etc.) over the course of a diurnal cycle and with respect to various backgrounds An integrated controlled experiment of simulated coal fires was conducted on 23rd and 24th of July 2002. A simulation of coal fires has never been done by other coal fire researchers and is unique in its design. Also detailed temperature measurements of coal fires have not been reported about. The advantage of simulated coal fires versus natural coal fires is the fact that simulated coal fires under easily controllable conditions can be investigated in more detail than in the field. Firstly, materials used (background materials and the coal itself) are very homogeneous and temperature variation according to changes in background material or coal layering density etc. can be excluded. Furthermore, temperatures can be measured over the course of the night, which is difficult to achieve in dangerous coal fire terrain in-situ. Also, detailed inside-fire temperatures could be collected through the special set up of the experiment. In the field, inside-fire temperatures can only be obtained at places, where cracks in the bedrock allow a "direct access" to the fire. This is rarely the case. Additionally the simulated fires could be observed with a thermal line scanner mounted on an observation tower as well as with a thermal scanner from an airplane. Due to logistic limitations these two measurement options would not have been possible in-situ for the coal fires in China (which we usually investigate).

The purpose of the work is thus to receive more detailed temperature information about coal fires that we could not collect at real coal fires in-situ (e.g. the inside-fire temperatures). Furthermore, the applicability of thermal line scanner instruments and thermal aerial survey should be tested. Generally speaking, the presented research belongs to the category of basic research – all aiming at a better understanding of coal fire thermal patterns, separability of thermal anomalies and background and the supply of data for future modelling. Currently, the topic of coal fires raises increased awareness in public and scientific media, since possible extinction of fires could contribute to certified emissions trading within the framework of the Kyoto Protocol and future protocols to follow. Currently, several researchers are involved in the question on how to define baselines for green house gas emission estimates. This tasks proves difficult since underground coal fires are not accessible, vary strongly in size and burning intensity and many questions are still unanswered. Thus, we believe that any additional information on coal fire temperatures and their distribution is needed.

During the experiment on July 23rd it was sunny and on July 24th it was cloudy. Two coal fires, simulating both a surface and an underground coal fire, were ignited at 9:00 in the morning of the first day and kept continuously burning until 14:00 in the afternoon of the following day. The fire's temperatures were measured on the ground using contact thermometers as well as non contact Raytec radiometers. Measurements were pursued in numerous spots on the surface and even within the fires as well as during numerous times of the analyses period. Additionally, a Raytec MP 50 Line Scanner, mounted on an observation tower, was tested for the recording of radiant temperatures of the fires. Furthermore, an airplane equipped with the Advanced BIRD Airborne Simulator (ABAS) sensor for detecting thermal anomalies passed over the test area 17 times at different flight heights. The ABAS sensor is an airborne sensor, which has the same configuration as the satellite sensor BIRD (Oettl et al., 2003).

2. Setting of the experiment

The coal for the experiment was high quality anthracite coal of similar composition as part of the coal in the Chinese coal fire areas, we usually investigate (Kuenzer et al., 2007a). As background material for the surface fire as well as for the covering of the subsurface fire a bright coarse grained quartz sand with a particle diameter of 0.1–0.5 mm was ordered. It was representative for the light coloured white to beige sandstone often overlaying the coal seams in our Chinese test areas.

The experiment was located at a sports field of the German Aerospace Centre, DLR, Oberpfaffenhofen, Germany. As shown in Fig. 2, an observation tower is located in the centre of the northern part of the test site.

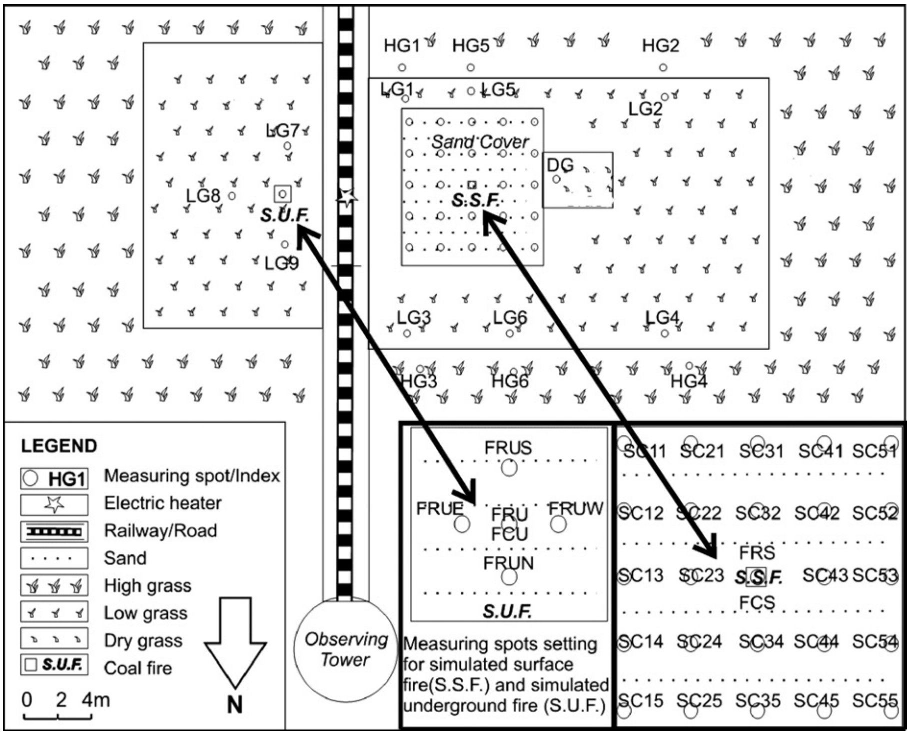

Fig. 2. Map of test site at DLR, Oberpfaffenhofen. Note that the left side is the eastern part of the test area and the right part is the western part of the test area since we visualized this map as observing the area from the observing tower. SUF: simulated underground fire. SSF: simulated surface fire. HG: high grass, LG: low grass. The magnified drawing in the lower right corner shows a more detailed setting of the two fires: the simulated underground fire left, and the simulated surface fire, right. Note that in the experiment set up an electric heater (star) is placed between those two fires for calibration purposes. FCU: Contact temperature for simulated underground coal fire in fire centre, FRUN, FRUE, FRUS, and FRUW radiant temperature measurement on top of the sand cone, facing to the North, East, South and West. FRU = Fire Radiant Temperature of underground fire on the surface. SC11–55: Measuring spots on the sand cover area of the simulated surface fire.

Thermal monitoring and camera equipment were placed about 10 m above the ground. A concrete path with railway tracks separates the test site into two parts: the eastern part and the western part. Both parts were covered by green grass with a height of 50 cm. We refer to it as'high grass'. The simulated underground coal fire was located in the eastern part and the simulated surface coal fire was located in the western part. They were 25 m away from the tower and 2 m away from edges of the concrete path. Around the fires, the grass was cut to 10 cm height. We refer to this second grass type as'low grass' (see Figs. 2 and 3).

The simulated surface fire was ignited in a metal wire container with dimensions of 0.5 m length, 0.5 m width and 0.5 m height. The container was fixed on a base supporter with a dimension of 1 m length, 1 m width and 0.5 m height. The container was constructed using thermal resistant material and was perforated to provide optimal air ventilation (see Fig. 3). An underground coal fire was simulated by covering a burning coal fire with a sand cone. This fire was held in a similar container with dimensions of 1 m length, 1 m width and 0.5 m height (see Fig. 4). The size of the container is four times as big as the one for simulating the surface fire. The big container could hold more coal, which could not only make the fire strong enough to not be extinguished by the sand cone, but also to make the fire last long enough for the measurement cycle. The underground container had an extra ventilation system, consisting of perforated tubes at the bottom of the box. These three tubes were 2.5 m long. They could transport air from outside the covering sand cone into the covered coal in case the fire would not get enough oxygen via the other pathways. However, it showed that these ventilation pathways were not necessary for the fire to remain burning. At 19:00 the fire was covered by a sand cone with a height of 0.5 m. This happened 10 h after the fire was ignited to ensure that the fire had a homogeneous inside temperature distribution.

A sand covered surface area with dimensions of 8.5 m × 8.5 m was placed on the western part of the test site to simulate a homogeneous environment. The sand was the same sand as that forming the underground coal

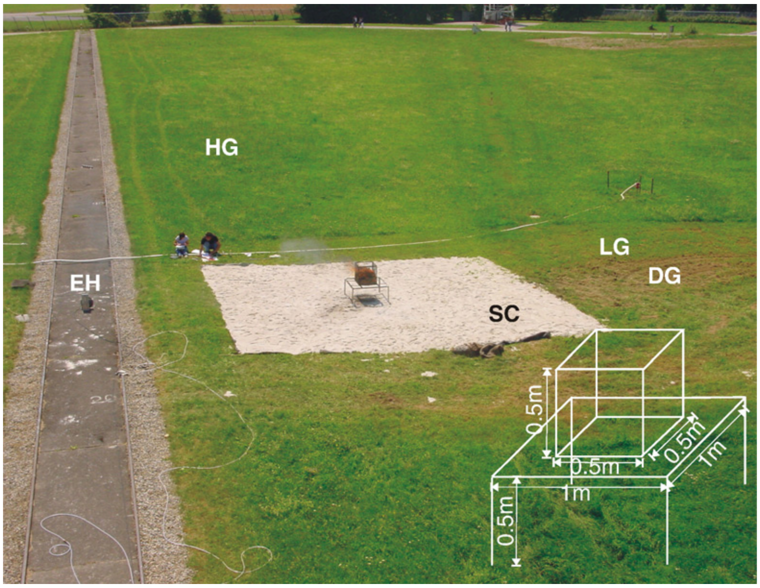

Fig. 3. Setting of the Simulated Surface Coal Fire. HG: High grass; LG: Low grass; DG: Dry grass; EH: Electric heater; SC: Sand cover. The sand cover occupies an area of 8.5 m × 8.5 m. 25 measuring spots named as SC11–SC55 as shown in Fig. 2 are located on it. The drawing in the lower right corner shows the dimension of the grill.

fire sand cone. The thickness of the sand cover was about 4 cm. The surface fire container was placed in the centre of this sand area (see FigFigs. 2 and 3). An electrical heater was placed in the middle of the two rail tracks. It was 25 m away from the observing tower and supplied a thermal calibration for the Raytec MP 50 Line Scanner.

3. Measurements

Ground temperature measurements were acquired using a contact thermometer and a radiant thermometer. The contact thermometer has three components: a thermal sensor, a connecting cable and a digital reading board. When the thermal sensor is put in a fire, the reading board

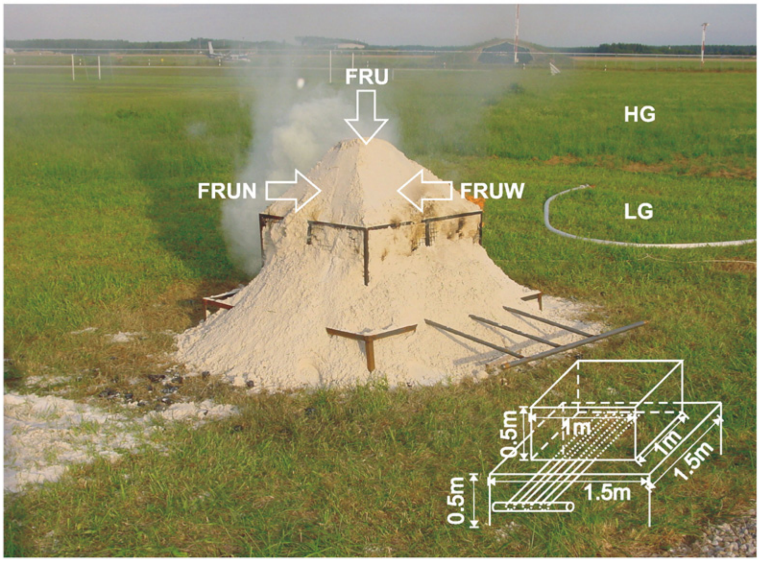

Fig. 4. Setting of the Simulated Underground Coal Fire. HG: High grass; LG: Low grass. The drawing in the lower right corner shows the dimension of the grill. Arrows point on the measuring spots on the sand cone, which have been described in Fig. 2.

gives a value of its temperature. It had been used for measuring the temperature inside the simulated surface fire and the simulated underground fire. The radiant thermometer is directed at the target, and the measuring spot on the surface is marked by a red laser marker. One receives readings of the radiant temperature for the red laser marked area. It had been used for measuring the surface radiant temperature of the simulated surface fire, the simulated underground fire, high grass, low grass, dry grass, and the sand covered area. Fig. 2 shows locations of measuring spots and their correspondent indexes using the radiant thermometer during the experiment. After the simulated underground fire was covered by the sand cone, it had 6 measuring spots located on the top of the sand cone (index: FRU), the centre of the fire measured by a contact thermometer (index: FCU), and centres of 4 cone slopes facing to the North, East, South and West (index: FRUN, FRUE, FRUS, and FRUW). High grass had 6 measuring spots (index: HG1-HG6). Low grass had 9 (index: LG1-LG9) and Dry grass had one (index: DG). In the sand covered area, there were 25 measuring spots (index: SC11–SC55), which were evenly distributed in the area with a distance between two spots of 2 m. The centre spot was the simulated surface fire. Each spot was marked to make sure that measurements were taken from the same point. Ground temperature measurements were acquired each hour from 11:00 to 14:00 of the next day (measurements were not started at 9:00, because it took some time to get the fire going).

The Raytec MP 50 line scanner took images of the fires from the observation tower. The Raytec MP 50 Line Scanner recorded temperatures of the fire areas 31 times between 14:20–20:37 on the first day and 62 times between 05:33–13:05 on the next day.

During the experiment, the ABAS sensor took airborne IR images of the test site. ABAS stands for Advanced BIRD Airborne Simulator. BIRD is a Bi-spectral InfraRed experimental Satellite, which was working between 2001 to 2004 (Oettl et al., 2003). The temperatures of the fires and background were also measured on the ground. During ABAS over-passes the ground temperature measurements of the sand cover area were taken at 5 measuring spots instead of 25 measuring spots because of time limits. The ABAS sensor was flown over the test site 17 times between 14:28–15:13 the first day and 05:41–06:23 and 07:57–08:31 on the next day, respectively. The ABAS main sensor payload consists of a two-channel infrared Hot Spot Recognition Sensor system (HSRS), and a Wide-Angle Optoelectronic Stereo Scanner(WAOSS-B). HSRS is a two-channel push-broom scanner with spectral bands in the mid-infrared (MIR:3.4–4.2 μm) and thermal infrared (TIR: 8.5–9 μm) spectral ranges.

4. Results

4.1. Temperatures of simulated coal fires and their thermal anomalies

The temperature inside the simulated surface fire (FCS) was measured 10 times using the contact thermometer between 11:00–19:00. The maximum temperature measured was 1080 °C. The minimum was 880 °C. The mean temperature was 983 °C (see Table 1) The standard deviation was 64 °C. Temperatures inside the simulated surface fire were completely independent from the outside air temperature (correlation factor 0.065).

Surface radiant temperatures for the simulated surface fire (FRS) have been measured 34 times using the radiant thermometer between 11:00 on the 23rd to13:00 of the following day. Within these 26 h, the maximum temperature measured was 900 °C. The minimum temperature was 309 °C. The mean temperature was 640 °C. Radiant temperature of the simulated surface fire could change up to 250 °C within one measurement time depending on spatial location. Radiant temperature for some parts of

Table 1
Temperature measurements in centigrade

Time	AT	FCS	FCU	FRS	Time	AT	FCS	FCU	FRS
11:15	24	880		313	1:45	15.7		950	400
12:15	29.4				2:45	15.7			500
12:52	25.7			309	3:45	14.9		850	600
13:55	24.9	957		500	4:45	15.5		1200+	17.8
14:20		920		600	5:42	15.3			700–900
14:28	30	994		650	6:01	15.2			45(NF)
14:38	26.3	937		680	6:08	15.6			700–900
14:47	26.3			49(NF)	6:16	15.2			700
14:59	28.8			33.8(NF)	6:24	15.3			650–900
15:05	24.4	1050		790	7:46	17.2			700–900
15:12	25.1	1050		600–850	8:04	17.8			750–900
16:36	25	1080		600–700	8:11	17.2			98(NF)
17:59	24.6	960		300–400	8:19	17.5			650–800
18:55	26	1005		670–780	8:25	17.2			700–900
19:15	21		842		8:39	17.3			700–900
19:50	19.5		1000	750	9:04	17.4			600
20:58	16.9		1070	800–900	10:08	18.2			600
21:45	14.5		890	360	11:07	19.6			550
22:46	14.4		900	600–700	12:05	19.8			500–600
23:45			870	600	13:10	20.8			860
0:45	15		970	600–700					

AT: Air temperature; FCS: Temperature inside the simulated surface fire measured with a contact thermometer; FCU: Temperature inside the simulated underground fire measured with a contact thermometer. FRS: Surface radiant temperatures for the simulated surface fire measured with a Raytec. NF: Temperature of the sand cover, where fire is removed away for a while as described in the text.

the fire was 650 °C, while at the same time, for other parts it was 900 °C (see Table 1). The surface radiant temperature of the simulated surface fire was also dependent on the inside fire temperature. Their correlation factor was 0.68.

The simulated surface fire was moved away from its original place 4 times during the experiment at the time of 14:47, 14:59, 06:01 and 08:11. The fire was removed for only about 1 min to allow scanner measurements with and without the fires. This was done to investigate the behaviour of the background relative to the removal of the heat source. The radiant temperature of the sand on the fire spot was measured just a few seconds after the fire was moved, which were 49 °C, 34 °C, 45 °C and 98 °C respectively. Before the removal they were 135 °C, 102 °C, 109 and 160 °C The correspondent air temperatures (AT) were 26.3 °C, 28.8 °C, 15.2 °C, and 17.2 °C. Measurements at 14:47 and 14:59 showed that the temperature of the thermal anomaly formed by the surface fire drops rapidly when the surface fire was moved away.

After the simulated underground fire was covered by the sand cone, temperature inside it (FCU) had been measured 10 times using the contact thermometer from 19:00 to 05:00 of the next day. The minimum temperature measured was 842 °C. The mean temperature was 954 °C. The standard deviation was 112 °C. During the last measurement, the thermal sensor melted and the thermometer broke. The melting temperature of the thermal sensor is 1200 °C, which means that temperature inside the simulated underground fire reached over 1200 °C.

The surface radiant temperature of the 5 measuring spots (FRU, FRUN, FRUE, FRUS, and FRUW) for the simulated underground fire was measured 11 times using the radiant thermometer from 19:15 to 04:45 of the next day. The results are shown in Fig. 5. It can be seen that at 19:15, which is just a few seconds after the sand cone had been built, the top measuring spot of the sand cone (FRU) had a 3.5 °C lower temperature than the maximum temperature of the background. Here we use the four corner measuring spots SC11, SC15, SC51, and SC55 of the sand layer of the surface fire (see Fig. 2) as the background (they are not influences by the surface fire, which will be demonstrated later). After 35 min, at 19:50, it had a 1.5 °C higher temperature than the maximum temperature of the background. This high temperature could be considered as a thermal anomaly induced by the coal fire. The thermal anomaly had a temperature ranging 1.5 °C to 4.2 °C higher than the maximum temperature of the background. The average is about 3 °C. The reason that the thermal anomaly was formed so rapidly is that the sand cone had a high porosity, which favours air ventilation and heat transfer through convection. The highest

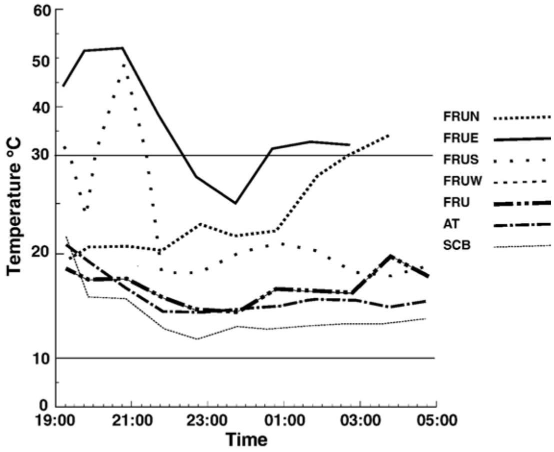

Fig. 5. Surface Temperature of the Simulated Underground Coal Fire. FRUN: Radiant temperature measured at the centre of the North Slope of the sand cone; FRUE: East slope; FRUS: South slope; FRUW: West slope; FRU: Top as shown in Fig. 4; AT: Air temperature; SCB: Background temperature from the sand cover in the simulated surface fire area as SC shown in Fig. 3. From 19:30, the temperature of the background was the lowest. Heat from the fire transferred to the top of the sand cone within 1 h. The top of the sand cone is warmer than the background by an average temperature of 3 °C. Note that the *y*-axis between 10–30 °C is extended (enlarged) to better visualize the parallel graphs of FRU, AT and SCB.

temperature difference of 6.7 °C between the fire thermal anomaly and the background maximum occurred at 03:45 due to a collapse of a cone slope. Radiant temperatures for measuring spots FRUN, FRUE, FRUS, and FRUW showed higher values than that of the top measuring spot FRU, because they were closer to the fire (sand cover on the slopes of the cone was thinner). Temperatures for FRUE, FRUS, FRUW showed big variances. They ranged from 20 to 50 °C. Heat coming from the side of the fire container influenced the measurements and it also has to be kept in mind that the sand cone is not completely stable. As the coal burns, volume loss occurs and the sand will slightly shift (see Fig. 4).

4.2. Temperature of background materials

If we investigate thermal anomalies we need a reference that anomalies can be considered anomalous against. Each fire thermal anomaly can only be detected (in-situ or in thermal imagery) if the difference to the background is pronounced enough. Thus background measurements act as a kind of standard and also reflect the natural temperature variation of the common surfaces in real coal fire areas.

Fig. 6 shows diurnal radiant temperature variations for high grass (HG), low grass (LG), dry grass (DG), and

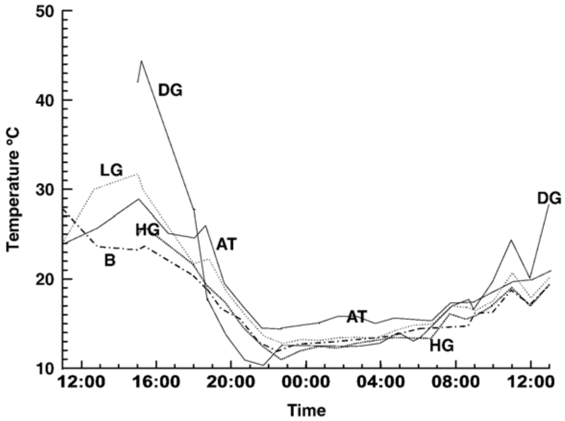

Fig. 6. Diurnal radiant temperature variations for different materials. AT: Air temperature; HG: High grass; LG: Low grass; DG: Dry grass. B: sand cover background as shown in Fig. 3. All surfaces show the same trend: High radiant temperature during daytime and low temperature during night-time.

air temperature (AT). Data on diurnal changes in radiant temperature for these materials are calculated from the averages of all measurements. As fire background temperature the temperatures resulting from the average measurements of the sand cover were taken (B). The most rapid temperature changes, shown by steep curves, occur near dawn and sunset. Low grass always showed higher temperatures than high grass. Dry grass showed cooler temperatures than low grass during night-time, but warmer temperatures than low grass during daytime. This is due to a higher biomass and thus water content in the high grass, which leads to a higher thermal inertia of these areas. The higher the water content of an object the higher its thermal inertia, meaning the higher its resistance for a heating of 1 °C, e.g. water surfaces have a lower diurnal temperature amplitude than land surfaces. The curve for radiant temperature of the sand cover is located between the curves for high grass and low grass during night-time. During daytime, high grass and low grass are warmer than the sand cover (with one exception). During the day time, the temperature difference among these background materials is high, while at in night-time, the difference is low. The curves for all these materials have the same trends. The correlation between air temperature and the sand cover is 0.90. The correlation factor between sand cover and low grass is 0.92. Between high grass and low grass it is 0.98. Concluding we can say that all background material follow the same trend, which goes in accordance with the outside air temperature. Night-time is more suitable for background-anomaly separation since the variation of background temperatures is less accentuated.

4.3. Temperature distribution of the surface fire's background sand layer

The sand layer can be considered as a homogenous area. In this 8.5 m*8.5 m area, 25 measuring spots (SC11–SC55) were set (see Fig. 2). Radiant temperatures for these observing spots were measured every hour during the experiment. The uncovered surface fire itself was of course not measured for these background observations. The experiment setup (see Fig. 3) allowed to measure underneath the container holding the fire. According to the distance to the fire, these measurements were grouped into 5 groups (see lower right area of Fig. 2). Group I includes the measuring spots SC32, SC23, SC43, and SC34, which were 2 m away from the centre of the fire. Group II includes the measuring spots SC22, SC42, SC24, and SC44, which were 2.8 m away from the centre of the fire. Group III includes SC31, SC13, SC53, and SC35. They were 4 m away from the centre. Group IV includes SC12, SC21, SC41, SC52, SC54, SC45, SC25 and SC14. They were 4.5 m away from the centre. Group V includes 4 corner spots (SC11, SC15, SC51 and SC55). They were 5.6 m away from the centre. Diurnal mean radiant temperature variations for these five groups are shown in Fig. 7. It can be seen that the radiant temperature for group one was always higher than that for other groups. From 18:00 to 13:00 the next day the radiant temperature for group 2 was higher than that for group 3, 4 and 5. From 16:30 to 09:00 the next day the radiant temperature for group 3 was higher than that for group 4 and 5. The diurnal radiant temperature for group 4 was almost the same as that for group 5. This can be interpreted as following. The simulated surface coal fire can heat the surroundings through radiation and wind-induced convection in a proximate distance of 2 m and forms a 1 °C difference thermal anomaly (2 measurements out of 21 were smaller than 1 °C). Other sources for the anomaly can be excluded — the sand layer was homogeneous, the measuring area was completely flat and the measuring device calibrated and temperature measurements were actually always recorded even with two radiance thermometers, which showed no difference during the whole measuring period. In our case the heat from coal fires does not influence areas at a distance further away than 4.5 m. Group 4 and group 5 can be considered as background. The heating extent of the fire can sometimes reach 2.8 or 4 m and forms a thermal anomaly with temperature difference less than 1 °C.

Fig. 8 shows 4 diurnal maps of radiant temperatures for the background sand cover below the fires. The maps indicate the thermal anomalous pattern formed by the

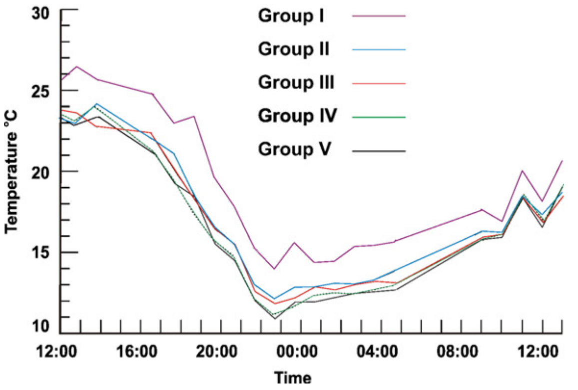

Fig. 7. Diurnal Radiant Temperature Variations for Measurements with Different Distance to the Coal Fire. Group I: Measuring spots 2 m away from the fire; Group II: 2.8 m; Group III: 4 m; Group IV: 4.5 m; Group V: 5.6 m. Thermal anomalies caused by the fire can not reach further than 4.5 m.

subsurface coal fire on the ground below the fire container. The axis of the high values (arrows) shows the dominant heat transfer directions. Probably caused by wind influence (because other influences can be excluded), the dominant heat transfer directions varied to almost all directions. Although the radiant temperatures are higher when the measuring spots are closer to the fire, the pixels close to the fire centre never formed a perfect circle (or a concentric temperature pattern of gradual temperature decrease with distance from the fire centre). We think that a thermal anomaly is formed not through radiation, but by wind driven convection of heat with shifting air masses. Of course no real-world conditions allow for the measurement of surfaces below coal fires. However, the conclusions drawn from the measurements are meaningful also for real world conditions. Fig. 8 indicates that convection plays the major part for the irregularity of the thermal anomalies. This means that the shape and extent of thermal anomalies mapped in-situ also strongly depends on the weather situation.

From Fig. 8 we can draw a very important conclusion. The assessment of coal fire dynamics is very difficult. As we can see from Fig. 8 the manifestation of the coal fire anomaly with regard to the background surface is not exclusively depending on the fire's intensity, but also on factors like wind direction and speed, which is the only factor that varied during the experiment. The fire represented in Fig. 8 has always been stable. Comparing the 17:50 result (with three anomalous hot pixels) with the 13:00 result on the next day (2 outstanding pixels) does not allow for the conclusion that the fire has shrank or changed. This finding is very important with respect to airborne and satellite based remote sensing research undertaken, where some authors conclude from multi-date imagery (e.g. 1995 and 1999) that a fire has grown, shrank or moved a certain direction (Prakash and Gupta, 1999, Prakash et al., 1995).

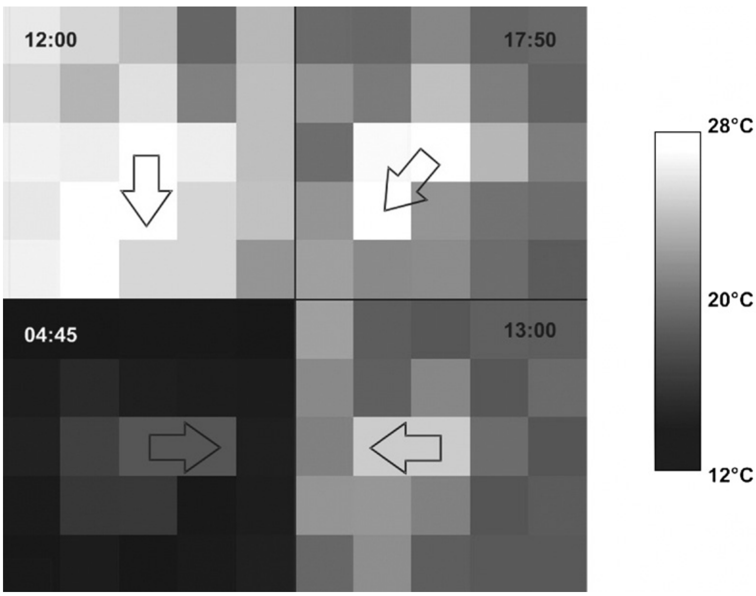

Fig. 8. Diurnal Maps of Radiant Temperatures for the Sand Cover as shown in Fig. 3 derived from point measurements (SC11–SC55 in Fig. 1) with a radiometer. Arrows indicate the main heat transfer directions. These shifts occur randomly and mainly seem to depend on outside wind.

4.4. MP 50 line scanner images of coal fires

The MP 50 line scanner is a stationary scanner. The radiation transmitted through an IR filter is focused onto a detector that converts the radiation into an electric signal. The resulting image records radiant temperature for targets in decimal degrees. A pixel will be saturated at 300 °C. The MP 50 line scanner was set 25 m away from the fires and 10 m above the ground. The resulting images have a spatial resolution of 5 cm.

Fig. 9 shows a series of the MP 50 line scanner images acquired at 14:34 and 20:29 on the first experiment day as well as on 05:33, 08:01, 11:01, and 13:05 on the next day. The images cover an area of the simulated underground coal fire and its surroundings, including the electric heater that served as a standard thermal emission source with a certain fixed temperature. The simulated underground coal fire was covered by the sand cone from 19:00 of the first day to 08:30 of the next day.

In all images the fire formed a thermal anomalous cluster occupying a lot of pixels in all images. The thermal anomalous cluster was so outstanding that it could be easily separated from the background. It saturated in Fig. 9 a, and f, where the simulated surface fire is not covered yet and respectively uncovered again. The electric heater forms a constant anomaly always saturating.

The differences between Fig. 9-a to f are obvious. In Fig. 9-a the fire is still uncovered, burning at full intensity, and reaching saturation in the line scanner imagery. In figure b, which was acquired 1 h and 29 min after the fire had been covered, the thermal anomaly is already much weaker. It has split into a bimodal anomaly, which might result from uneven sand layering density of the covered fire and existing ventilation channels. However, the anomaly weakens and only forms a very subtle anomaly against the background at 5:33 am the next day (see Fig. 9-c). The anomaly is more accentuated at 8:01, which is due to increasing instabilities in the sand cone. 2 h and 31 min after the burning coal was uncovered again the anomaly picks up again and increases in strength (Fig. 9-e), until reaching its original strength before the covering process (Fig. 9-f). The time lag between the uncovering and the anomaly reaching its full manifestation depends on ventilation, which increases the burning

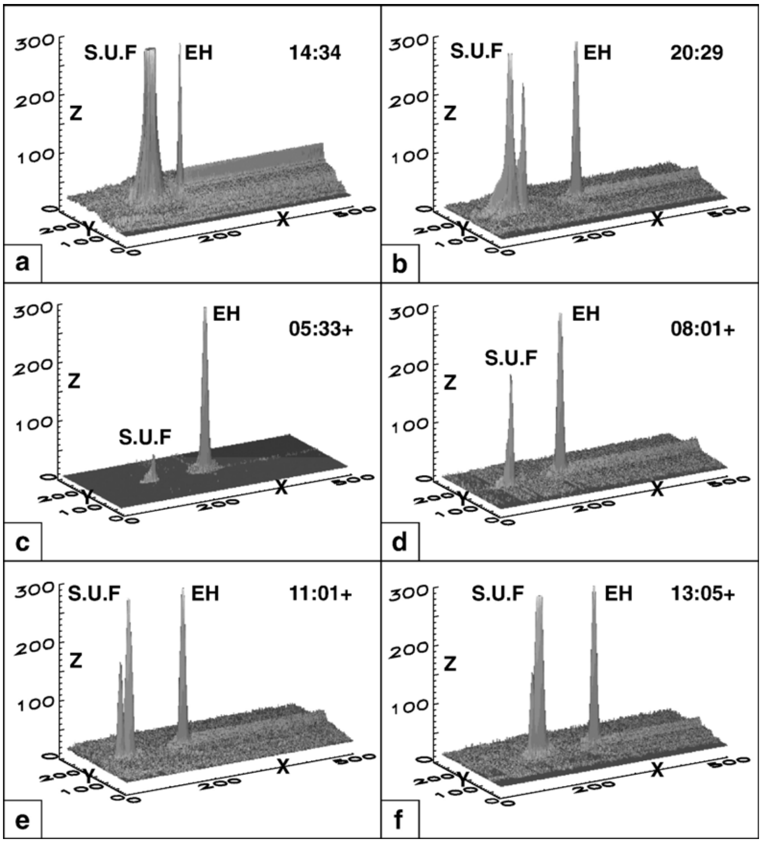

Fig. 9. MP 50 line scanner images. *X*: Rows; *Y*: Columns; *Z*: Temperature (°C); S.U.F.: Simulated underground coal fire; EH: Electric heater. The coal fire with a dimension of 1 m * 1 m forms an outstanding thermal anomalous cluster in MP 50 line scanner images, whose spatial resolution is 5 cm.

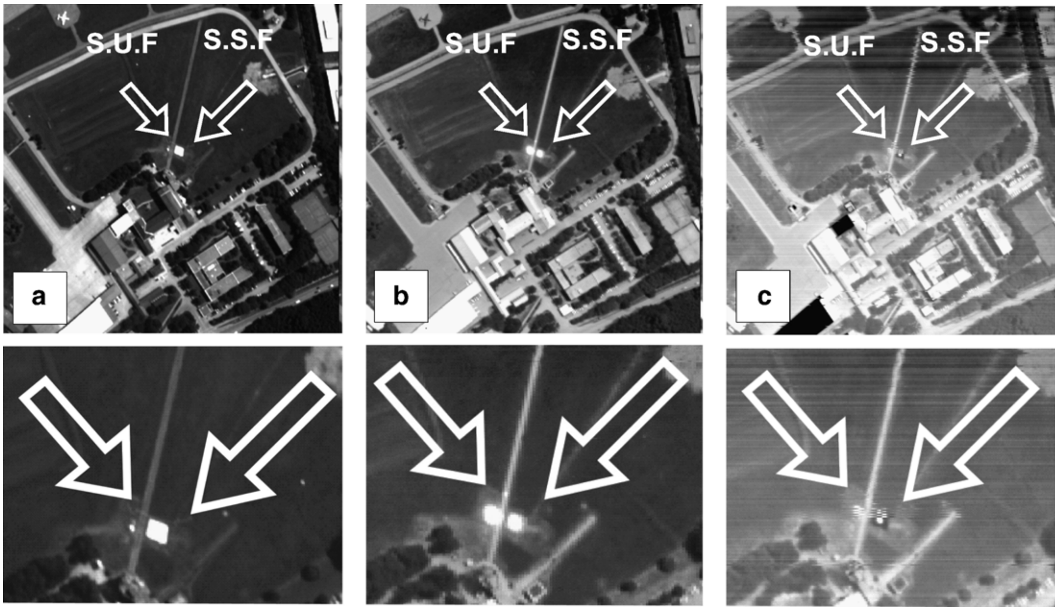

Fig. 10. ABAS thermal scanner image acquire on July 23rd 2002 at 15:11 pm. a: NIR domain at 0.89 μm, b: MIR domain at 3.8 μm and c: TIR domain at 8.8 μm. Images in the second row are the zooms of the areas of interest.

intensity of the fire. When the fire is uncovered the coal will be exposed to air. With increasing ventilation and wind the burning process will speed up again.

Concluding we can say that a thermal line scanner represents changes in coal fire thermal anomalies and temperature distribution very accurately. The resolution of the images is very high (5 cm). To mount a scanner on a observation rack would even be feasible in complicated coal fire terrain. Thus, line scanners could be employed to monitor coal fire extinction activities and ensure that coal fires do not flare up again.

4.5. ABAS images of the simulated coal fires

The ABAS sensor flew over the simulated coal fires of the experimental test site several times during the 2 days. However, due to strong distortions in geometry and radiometric instabilities at that time only few images provided useful for later analyses. Fig. 10 shows black and white image acquired on July 23rd at 15:11 in the afternoon. Fig. 10-a represents the area as seen in the reflected 0.89 μm band, which is more or less a visual representation of the experimental site. Note that the sand cover of the sub-surface fire can be seen as a small light dot left of the railway track. The background sand layer of the surface fire can be seen as a light square (compare also with Figs. 2, 3, and 4). In Fig. 10-b we see the mid-infrared image acquires at 3.8 μm wavelength. In this wavelength domain very bright spots indicate very hot spots. Note that the sub-surface fire anomaly seems a little bit smaller (right hot spot). This is because the surface fire is smaller in dimensions (compare Figs. 3 and 4) and both fires are uncovered (the sub-surface fire was covered with the sand cone only at 19:00). Fig. 10-c represents the emission pattern in the thermal domain at 8.8 μm. Bright areas are regions of high temperature, while dark regions exhibit low temperatures. As expected, vegetation (trees) emits the lowest temperatures. The two fires can be spotted as small hot spots, which are not as outstanding as in the mid infrared domain.

5. Conclusions

From the conducted two day experiment of simulated coal fires under outside simplified conditions we can draw the following conclusions.

1. The inside temperature of surface coal fires is independent of the surrounding air temperature, while the fire's surface radiant temperature shows a high correlation with inside fire temperatures. In situ inside fire temperatures should thus be independent of season. Since the surface temperature should stay constant while the background varies, coal fire observations at low temperatures (winter time or night-time) should be favoured for maximum contrast of thermal anomalies.
2. The stability of a thermal anomaly formed on the fire's background (sand layer) is relatively low. If the

fire is moved the related anomaly in the surrounding material will also disappear fast. It has to be investigated if this also applies under in-situ conditions at real coal fires. However, this can only be assessed if a coal fire is extinguished relatively fast.
3. The interior temperature for a simulated surface coal fire averages 1000 °C. For the simulated underground coal fire, the interior temperature could reach above 1200 °C. The surface radiant temperature for the simulated coal fires range from 300 to 900 °C.
4. Within 1 h heat could be transported through a 0.5 m high sand cone to the surface and form a thermal anomaly with a temperature about 3 °C higher than that of the background. With passing time the temperature difference will increase — however, the subsurface anomaly will always be much weaker than the one resulting from an uncovered coal fire. Even though the inside-fire temperature of the subsurface fire is higher, the cover leads to a weakened thermal anomaly.
5. Diurnal radiant temperature variations for high grass, low grass, dry grass, and the sand cover showed the same trend. During day time, the temperature difference among these background materials is high, while during night-time, the differences are low. Diurnal patterns depend on albedo and thermal inertia. The correlation between outside air temperatures and the material's temperatures is high.
6. The simulated surface coal fire can heat the surroundings through radiation and wind-driven convection in a distance of approximately 2 m and form a 1 °C difference thermal anomaly. However, the fire does not form a thermal anomaly further away than 4.5 m. The influencing distance of the fire is dependent on its temperature and weather conditions (Fig. 7). Heat from the simulated surface fire was transported mainly by wind-driven convection, not radiation. Main heat transfer directions vary continuously and are most likely depending on wind direction and speed.
7. In spatial thermal data (e.g. airborne thermal imagery or satellite thermal imagery) it is not scientifically reasonable to interpret the heat distribution pattern within pixels as a representation of a fire's dynamics. The growth or shrinking of an anomaly from one point in time to another can be induced by various phenomena. These changes can be weather related or related to changes in the composition/density of overlaying materials.
8. The coal fire with a dimension of 1 m × 1 m forms outstanding thermal anomalous clusters in MP 50 line scanner images, whose spatial resolution is 5 cm. We could observe clear relationships between the results of line scanner images and the covering and uncovering process of the simulated sub-surface fire. Line scanner might be a powerful equipment to investigate individual fire's in situ – especially if thermal cameras are not available. Line scanner imagery might be a powerful and cost efficient tool for monitoring of extinction activities.
9. Coal fire related thermal anomalies can be picked up in thermal scanner ABAS data. It is obvious that the very hot fires create a larger hot spot in mid infrared data than in data of the thermal domain. This is due to the shift of maximum emission to shorter wavelength with increasing temperature (Wien's law). Thus, we can conclude that very hot coal fire are represented better in mid-infrared data, while "colder" coal fires are represented better in thermal domain data. Detection and manifestation of this signal of course also depends on spatial resolution.

Overall, our findings demonstrate that even under strictly controlled experimental conditions especially sub-surface coal fires exhibit a strongly fluctuating behaviour probably influenced by weather conditions and the stability and fracturing of overlaying material.

Acknowledgements

The authors thank all the numerous people supporting the set up of the experimental test site in DLR Oberpfaffenhofen. Further thanks go to all scientists of the Sino-German coal fire research initiative for the long-term and ongoing exchange of ideas on the topic of coal fires.

References

Banerjee, S.C., 1982. A theoretical design to the determination of risk index of spontaneous fires in coal mines. Journal of Mines, Metals and Fuels 30, 399–406.
Banerjee, S.C., Nandy, D.K., Banerjee, D.D., Chakravorty, R.N., 1972. Classification of coal with respect to their susceptibility to spontaneous combustion. Transactions of the Mining and Metallurgical Institute of India 59 (2), 15–31.
Bylo, Z., 1960. The role of sulphonation in the spontaneous ignition of coal. Serie des Sciences Techniques 8 (2), 107–114.
Chaiken, R.F., Brennan, R.J., Heisey, B.S., Kim, A.G., Malenka, W.T., Schimmel, J.T., 1998. Problems in the control of anthracite mine fires: a case study of the Centralia Mine Fire. Report of Investigations 8799 of the United States Department of the Interior. Pittsburgh, USA, 68 pp.
Chen, L., 1997. Subsidence assessment in the Ruqigou Coalfield, Ningxia, China, using a geomorphological approach. Master thesis at ITC. Enschede, Netherlands, p. 130.
Coates, D.A., Heffern, E.L., Naeser, C.W., Reiners, P., 2005. Coal bed fires — a long history of burning and change in the Northern Great Plains. Proceedings of the International Conference on Coal Fire Research, 29.11.-01.12.2005 Beijing, pp. 98–101.

Dai, S., Ren, D., Tang, Y., Shao, L., Li, S., 2002. Distribution, isotopic variation and origin of sulfur in coals in the Wuda coalfield, Inner Mongolia, China. International Journal of Coal Geology (57), 237–250.

Ellyett, C.D., Fleming, A.W., 1974. Thermal infrared imagery of the Burning Mountain coal fire. Remote Sensing of Environment 3 (1), 79–86.

Fisher, W., Knuth, W., 1968. Detection and delineation of subsurface coal fires by aerial infrared scanning. Geological Society America 115, 67–68.

Giglio, L., Kendall, J.D., Justice, C.O., 1999. Evaluation of global fire detection algorithms using simulated AVHRR infrared data. International Journal of Remote Sensing 20, 947–1985.

Glover, L., 1998. Burning Beneath the Surface. Tribune Review Publishing, USA. (May 3, 1998).

Guan, H., 1989. Applications of remote sensing techniques in coal geology. Acta Geologica Sinica 2, 253–269.

Knuth, W.M., Fisher Jr., W., Stingelin, R.W., 1968. Detection, delineation and monitoring of subsurface coal fires by aerial infrared scanning. Geographer HRB-Singer, Inc., a subsidiary of the Singer Company, state College, Pennsylvania, USA, pp. 877–881.

Kuenzer, C., 2005. Demarcating coal fire risk areas based on spectral test sequences and partial unmixing using multi sensor remote sensing data. Ph.D. thesis, Technical University Vienna, Austria, 199 pp.

Kuenzer, C., Zhang, J., Tetzlaff, A., Voigt, S., Van Dijk, P., Wagner, W., Mehl, H., 2007a. Uncontrolled coal fires and their environmental impacts: investigating two arid mining environments in north-central China. Applied Geography 27, 42–62.

Kuenzer, C., Wessling, W., Zhang, J., Litschke, T., Schmidt, M., Schulz, J., Gielisch, H., Wagner, W., 2007b. Concepts for green house gas emission estimation of underground coal seam fires. Geophysical Research Abstracts of the EGU General Assembly 2007, 16.4.-20.4. Vienna, Austria. 2 pp.

Kuenzer, C., Zhang, J., Li, J., Voigt, S., Mehl, H., Wagner, W., 2007c. Detection of unknown coal fires: synergy of coal fire risk area delineation and improved thermal anomaly extraction. International Journal of Remote Sensing 28, 4561–4585.

Kuenzer, C., Hecker, C., Zhang, Wessling, S., Wagner, W., accepted for publication. The potential of mulit-diurnal MODIS thermal bands data for coal fire detection. International Journal of Remote Sensing. doi: 10.1080/01431160701352147

Lapham, D.M., Barnes, J.H., Downey, W.F., Finkelman, R., 1980. Mineralogy associated with burning anthracite deposits of Eastern Pennsylvania. Mineral Resource Report 78 of the Pennsylvania Geological Survey. 82 pp.

Li, D.X., 1985. Applied study of airborne remote sensing in Taiyuan coalfield, China. Internal Report of the Remote sensing centre of the ministry of coal industry, Xian, China, pp. 3–10 (in Chinese).

Litschke, T., Wiegand, J., Schloemer, S., Gielisch, H., Bandelow, K.F., 2005. Detailed mapping of coal fire sites in combination with in-situ flux measurements of combustive gases to estimate gas floor balance and fire development. Proceedings of the International Conference on Coal Fire Research, 29.11.-01.12.2005 Beijing, pp. 161–163.

Livingood, M., Winicaties, J., Stein, J., 1999. Centralia mine fire analysis: presence of sulfur-bearing mineral deposits at thermal vents. Research paper at West Chester University, Pennsylvania, USA. 9 pp.

Lohrer, C., Schmidt, M., Krause, U., 2005. Influence of environmental parameters on the self ignition of coal. Proceedings of the International Conference on Coal Fire Research, 29.11.-01.12.2005 Beijing, pp. 110–112.

Mansor, S.B., Cracknell, A.P., Shilin, B.V., Gornyi, V.I., 1994. Monitoring of underground coal fires using thermal infrared data. International Journal of Remote Sensing 15 (8), 1675–1685.

Masalehdani, M.N., Potdevin, J.L., Cazier, F., Courcot, D., Paquette, Y., 2005. Coal waste heap fires — emission of toxic gases and condensation minerals, Northern France measurements and analyses. Proceedings of the International Conference on Coal Fire Research, 29.11.-01.12.2005 Beijing, pp. 101–103.

Moxham, R.M., Greene, G.W., 1967. Infrared surveys of coal mine fires in the anthracite and bituminous fields, Pennsylvania. USA, Geological Survey Inter-Agency Report BM-2, U.S. Bureau of Mines. 67 pp.

Oettl, H., Briess, K., Lorenz, E., Oertel, D., Shrbek, W., Walter, I., Zhukov, B., 2003. The disaster,'fires', its detection and means to improve information. Space Technology 23 (4), 249–256.

Pennig, L., 2003. Vergleich zweier Kohlebrandregionen in Nordchina mit Hilfe von Fernerkundungs-daten und GIS. Master Thesis at the University of Jena, 90 pp.

Prakash, A., Gupta, R.P., 1998. Land-use mapping and change detection in a coal mining area – a case study in the Jharia coalfield, India. International Journal of Remote Sensing 19 (3), 391–410.

Prakash, A., Gupta, R.P., 1999. Surface fires in Jharia Coalfield, India—their distribution and estimation of area and temperature from TM data. International Journal of Remote Sensing 20 (10), 1935–4619.

Prakash, A., Saraf, A.K., Gupta, R.P., Dutta, M., Sundaram, R.M., 1995. Surface thermal anomalies with underground fires in Jharia coal mine, India. International Journal of Remote Sensing 16 (2), 2105–2109.

Saraf, A.K., Prakash, A., Sengupta, S., Gupta, R.P., 1995. Landsat-TM data for estimating ground temperature and depth of subsurface coal fire in the Jharia coal field, India. International Journal of Remote Sensing 16 (12), 2111–2124.

Schmugge, T.J., Becker, F., Li, Z.L., 1991. Spectral emissivity variations observed in airborne surface temperature measurements. Remote Sensing of Environment 35 (2), 95–104.

Tetzlaff, 2004, Coal fire quantification using Aster, ETM and Bird satellite instrument data. Ph.D thesis at the Ludwig Maximilians University Munich, Germany, 155 pp.

Walker, S., 1999. Uncontrolled fires in coal and coal wastes. International Energy Agency, IEA on Coal Research, London. 73 pp.

Wessling, 2007. The investigation of underground coal fires-towards a numerical approach for thermally, hydraulically and chemically coupled processes. PhD thesis at the Westfälische Wilhelms University of Münster, 157 pp.

Wessling, S., Litschke, T., Wiegand, J., Schloemer, S., Kessels, W., 2005. Simulating dynamic subsurface coal fires and its real life applications. Proceedings of the International Conference on Coal Fire Research, 29.11.-01.12.2005 Beijing, pp. 114–117.

Zhang, J., 2004. Spatial and Statistical Analysis of Thermal Satellite Imagery for Extraction of Coal Fire Related Anomalies. PhD thesis at the Technical University Vienna, Austria, 166 pp.

Zhang, J., Kuenzer, C., accepted for publication. Thermal Surface Characteristics of Coal Fires 1: Results of in-situ measurements. Accepted for publication at Journal of Applied Geophysics.

Zhang, X., Zhang, J., Kuenzer, C., Voigt, S., Wagner, W., 2004. Capability evaluation of 3–5 mm and 8–12,5 mm airborne thermal data for underground coalfire detection. International Journal of Remote Sensing 25 (12), 2245–2258.